PLoS PATHOGENS

Functional Amyloids Composed of Phenol Soluble Modulins Stabilize *Staphylococcus aureus* Biofilms

Kelly Schwartz[1], **Adnan K. Syed**[1], **Rachel E. Stephenson**[1], **Alexander H. Rickard**[2], **Blaise R. Boles**[1]*

1 Department of Molecular, Cellular, and Developmental Biology, University of Michigan, Ann Arbor, Michigan, United States of America, 2 Department of Epidemiology, University of Michigan, Ann Arbor, Michigan, United States of America

Abstract

Staphylococcus aureus is an opportunistic pathogen that colonizes the skin and mucosal surfaces of mammals. Persistent staphylococcal infections often involve surface-associated communities called biofilms. Here we report the discovery of a novel extracellular fibril structure that promotes *S. aureus* biofilm integrity. Biochemical and genetic analysis has revealed that these fibers have amyloid-like properties and consist of small peptides called phenol soluble modulins (PSMs). Mutants unable to produce PSMs were susceptible to biofilm disassembly by matrix degrading enzymes and mechanical stress. Previous work has associated PSMs with biofilm disassembly, and we present data showing that soluble PSM peptides disperse biofilms while polymerized peptides do not. This work suggests the PSMs' aggregation into amyloid fibers modulates their biological activity and role in biofilms.

Introduction

Staphylococcus aureus is the causative agent of numerous diseases ranging from relatively benign skin conditions to fatal systemic infections. Formation of bacterial biofilms on host tissues and implanted materials contributes to chronic *S. aureus* infections, as biofilms are exceptionally resistant to host immune response and chemotherapies [1]. Biofilms are multicellular structures encased in a matrix of proteins, polysaccharides, extracellular DNA, and other environmental factors [1,2]. Biomolecules that digest matrix components (e.g., proteases, DNases, and glycoside hydrolases) can disrupt established biofilms and render detached cells susceptible to antimicrobials [3,4,5,6,7].

The precise composition of the biofilm matrix varies greatly by strain, physiological state, and nutrient availability [5,8,9,10,11,12]. In this study, we examined how growth media affects the composition of the biofilm matrix. This led to the discovery of an extracellular fibril structure in *S. aureus* biofilms grown in a non-standard rich media. These fibers share morphological and biophysical characteristics with functional bacterial amyloids such as curli in *Escherichia coli* biofilms, TasA of *Bacillus subtilis*, and the Fap fimbriae in *Pseudomonas aeruginosa* [13,14,15,16]. Biochemical and genetic analysis revealed that these fibril structures are composed of small peptides called phenol soluble modulins (PSMs). Mutants incapable of producing PSMs formed biofilms that were susceptible to disassembly by enzymatic degradation and mechanical stress.

Previous work has demonstrated that PSMs are surfactant-like peptides that promote biofilm disassembly [17,18,19,20,21]; exhibit antimicrobial activity against niche bacteria [22,23,24]; hinder host immune response by recruiting and lysing neutrophils; and are abundant virulence factors produced by community-associated MRSA strains (CA-MRSA) [18,25,26,27]. The genes encoding the core family of PSM peptides are highly conserved across *S. aureus* strains: four are expressed from the alpha (α*psm*1–4) operon, two are expressed from the beta (β*psm*1&2) operon, and the delta hemolysin (*hld*) is encoded within the regulatory RNA, *RNAIII* [28,29,30]. The significance of the PSMs has only recently been investigated because the coding sequences of the α*psm* & β*psm* peptides are small enough to have eluded detection by conventional gene annotation programs, and they are still poorly annotated in public databases [29,30].

We have found that ordered aggregation of PSM peptides into amyloid-like fibers can abrogate the biofilm disassembly activity ascribed to monomeric PSM peptides [12,17,18,19,20,21]. Our findings suggest that PSMs can modulate biofilm disassembly using amyloid-like aggregation as a control point for their activity. This is the first report to identify and characterize extracellular fimbriae in the *S. aureus* biofilm, and our research could lead to new approaches in treating persistent biofilm associated infections.

Results

Biofilms grown in PNG media resist biofilm disassembly

Biofilms that persist in the human body are often resistant to conventional antimicrobial treatment prior to dispersal. To gain insight into how the *S. aureus* biofilm matrix affects disassembly under different growth conditions, we grew *S. aureus* flow cell biofilms with various lab media. Next we used enzymes known to target primary matrix components in order to test biofilm resistance (Fig. 1A & 1B). These enzymes include proteinase K (protein), DNaseI (DNA), and dispersin B (polysaccharide). By using a variety of degradative enzymes, we expected to observe complete biofilm eradication.

Author Summary

Most people know *Staphylococcus aureus* as a highly infectious "Super Bug", but many are not aware that *S. aureus* non-infectiously colonizes much of the population in the nose, among other bodily niches. It is not well understood how and why *S. aureus* is able to adapt and readily switch between the commensal and pathogenic lifestyle within the host; however, the capacity to accumulate into multicellular aggregates is a hallmark associated with both lifestyles. In this work, we demonstrate that *S. aureus* produces extracellular fibers in multicellular biofilm communities, and that these fibers help the bacterial community to withstand physical stresses. Surprisingly, these fibers consist of small peptides called phenol soluble modulins (PSMs) that have previously been implicated in biofilm disassembly and virulence. We demonstrate that accumulation of PSM peptides into fibers modulates their ability to disperse biofilms. Thus, PSMs fulfill dual and opposing roles that are modulated by amyloid-like aggregation. Staphylococci have never before been shown to produce this kind of extracellular structure, and our findings may have a profound impact on our understanding of *S. aureus* physiology. We have found that these structures are composed of known virulence factors, which indicates a common pathway between infectious and static lifestyles in the body.

Biofilms grown in tryptic soy broth supplemented with glucose (TSBg) rapidly disassembled after enzymatic treatment (Fig. 1A). However, biofilms grown in peptone-NaCl-glucose (PNG) media did not disassemble after the same enzymatic treatment (Fig. 1B).

We also assessed the ability of biofilms attached at the air-liquid interface of glass culture tubes to withstand exposure to an anionic surfactant, sodium dodecyl sulfate (SDS). Again, biofilms grown in TSBg were more sensitive to surfactant-mediated disassembly than those grown in PNG (Fig. 1C). We interpreted these results to be an indication that growth in PNG alters the matrix composition, increasing the biofilm's resistance to enzymatic degradation and surfactant dispersal. We hypothesized that a new, previously unaccounted for matrix component was influencing *S. aureus* biofilm integrity under these growth conditions.

Biofilms resistant to dispersal contain extracellular fibers

To investigate how biofilms grown in PNG media are able to resist disassembly, we grew biofilms in drip bioreactors under sensitive (TSBg) or resistant (PNG) conditions for five days. Biofilms were harvested and disrupted by vortexing and sonication. Transmission electron microscope (TEM) imaging of cells revealed the presence of extracellular fibers in enzyme-resistant biofilms (Fig. 2B), but not in enzyme-sensitive biofilms (Fig. 2A). The fibers had a central diameter of ~12 nm and were closely associated with bacterial cells (Fig. 2C). *S. aureus* has never before been shown to produce large, extracellular structures. Additionally, we observed identical fibers associated with biofilm cells in several lab strains (LAC, UAMS, MN8) and six clinical isolates (three nasal isolates and three blood isolates) by TEM, demonstrating that fiber formation is not specific to strain SH1000. Of note, we found that an *agr* quorum sensing mutant (SH1001) was unable to produce fibers (Fig. 2D).

## *Staphylococcus aureus* fibers are composed of phenol soluble modulins (PSMs)

The novel extracellular fibers isolated from robust biofilm matrices share morphological similarities with the bacterial
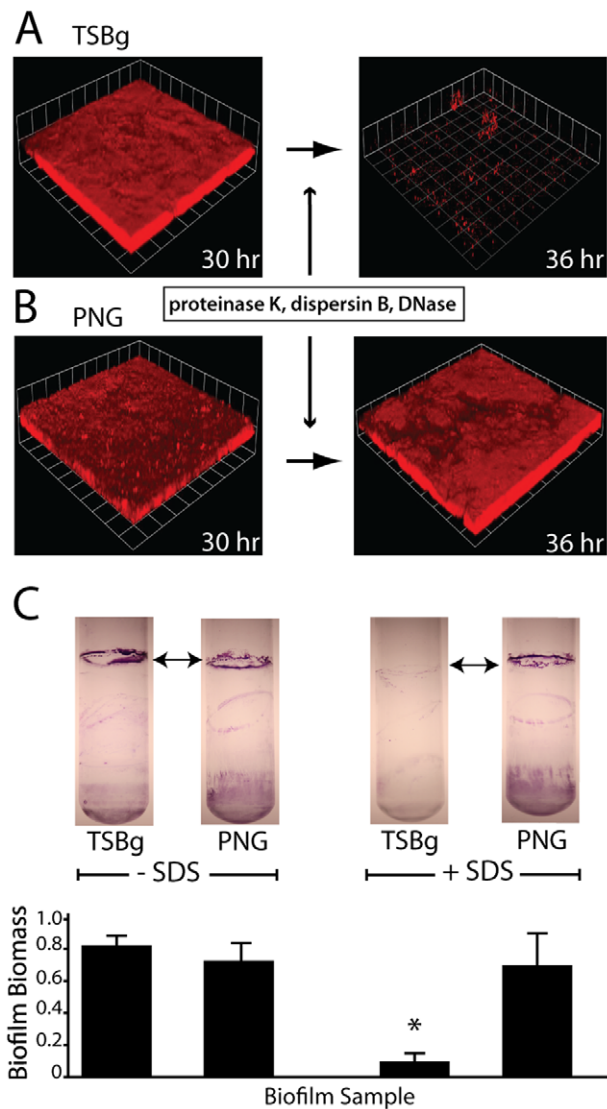
Figure 1. Growth media influences biofilm disassembly. Confocal micrographs of *S. aureus* SH1000 biofilms grown in TSBg media (A) for 30 hours readily disassemble upon exposure to biofilm matrix degrading enzymes proteinase K, dispersin B, and DNaseI at 0.2 µg/mL each. *S. aureus* biofilms grown in PNG media (B) for 30 hours fail to disassemble upon exposure to matrix-degrading enzymes. Images are representative of three separate experiments and each side of a grid square represents 20 µm. (C) Biofilms at the air-liquid interface of test tube cultures withstand 1% SDS exposure when grown in PNG media but disassemble when grown in TSBg. Top images show stained test tube biofilms; graph below is quantification of biofilm biomass. * P<0.002 compared to no SDS treatment.
doi:10.1371/journal.ppat.1002744.g001

functional amyloids curli in *E. coli* and TasA in *B. subtilis* [15,16]. Amyloid proteins form highly stable polymerized aggregates that exhibit well-defined biochemical and biophysical characteristics [14,31,32]. We hypothesized that our fibers were also functional bacterial amyloids. To identify the protein composing these fibers, we used two approaches to take advantage of the biophysical characteristics of functional bacterial amyloids.

Amyloid fibrils from bacterial biofilms were previously shown to be poorly soluble in sodium dodecyl sulfate (SDS) and do not migrate through polyacrylamide gels [33]. We therefore employed SDS-PAGE to isolate large insoluble structures. *S. aureus* biofilm
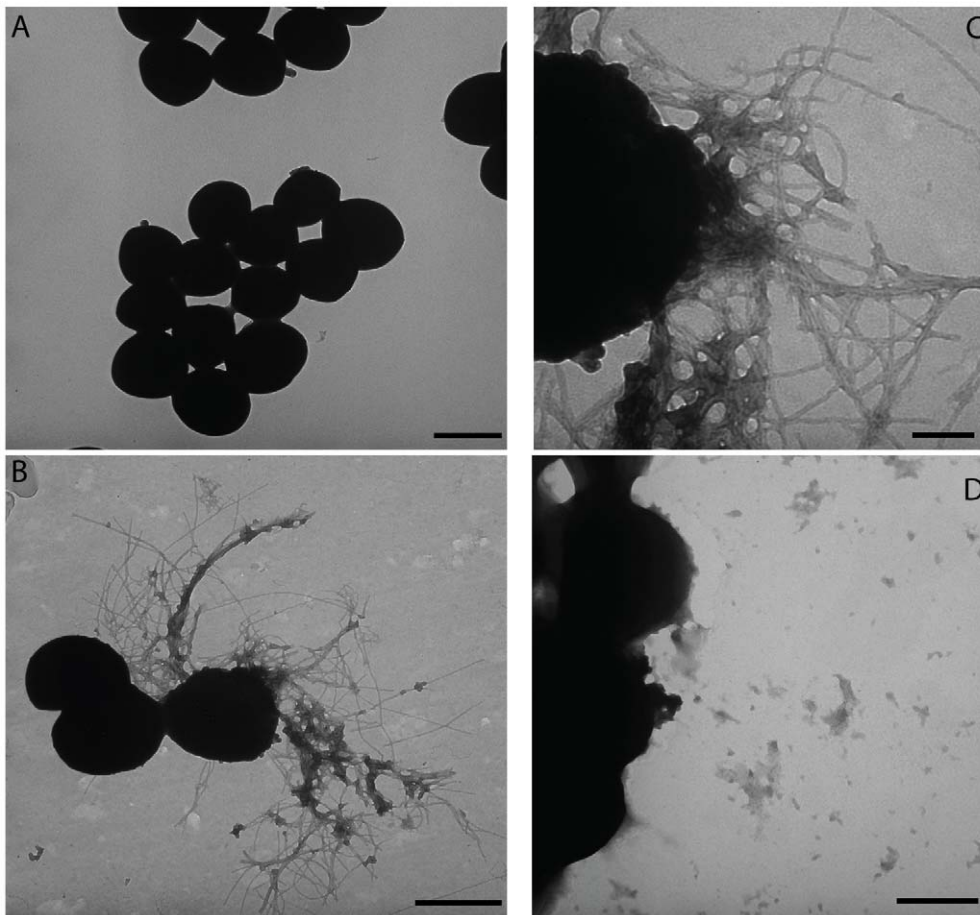
Figure 2. *S. aureus* produces extracellular fibers during biofilm growth in PNG media. TEM micrographs of cells from *S. aureus* SH1000 biofilms grown in TSBg medium (A) versus cells from biofilms grown in PNG media (B). High magnification reveals fibers are associated with the cell wall and approximately 12 nm in width (C). An *agr* mutant does not produce extracellular fibers (D). Bar length indicates 1 µm in A, B, and D, and 250 nm in C.
doi:10.1371/journal.ppat.1002744.g002

samples were grown in drip bioreactors for five days with PNG media or TSBg. These biofilms were harvested, homogenized, and lysed, and the lysates were run into a 12% SDS-polyacrylamide gel. Lysates from biofilms grown in PNG media retained insoluble material in the wells of the stacking gel while TSBg-grown lysates did not (Fig. 3A). The insoluble material retained within the wells of the stacking gel was recovered, treated with 100% formic acid (FA), then separated once more by SDS-PAGE alongside an untreated control (Fig. 3B). We observed protein enrichment in the FA-treated sample, and the four dominant bands were excised and analyzed via mass spectrometry (MS). Surprisingly, MS analysis identified the same peptides as being abundant in each sample, regardless of the band's migration through the gel matrix (Fig. 3B & 3D). These proteins were the alpha (αPSM) phenol soluble modulins and the *S. aureus* delta hemolysin (δ-toxin) (Fig. 4A & 4B).

An additional approach to identify the fiber subunit was to isolate fibers from biofilm cells using a tissue homogenizer (Fig. 3C), incubate fiber isolates for 48 hours at pH 2 with pepsin, and analyze the sample with MS. Again, we detected the same αPSM peptides present in the SDS-PAGE isolation plus two beta PSMs (βPSM) (Fig. 3D). αPSM3 was not identified in either preparation, but it should be noted that αPSM3's sequence contains several trypsin cleavage sites, so it is likely that it would

not be detected after extensive digestion. The same fiber isolation procedure revealed no visible fibers by TEM when biofilms were grown in TSBg.

We generated an ΔαβPSM double-knockout mutant and assessed fiber production. TEM analysis of biofilm cells revealed that this mutant did not produce fibers after five days of growth in PNG media (Fig. 5B) compared to the wildtype parent strain grown under the same conditions (Fig. 5A). In addition, fibers could be isolated from wildtype (Fig. 5D) but not mutant biofilms (Fig. 5E). Fiber production was complemented by expression of the α*psm* and β*psm* operons *in trans* (Fig. 5C & 5F).

PSM peptides form fibers similar to bacterial functional amyloids

We assayed synthetic PSMs peptides for their capacity to form fibers *in vitro*. To minimize the prevalence of polymeric "seed" complexes, all synthetic peptides were treated with HFIP/TFA and dried *in vacuo* prior to assay [34]. Incubation of the seven previously identified PSM peptides (αPSMs1–4, βPSMs1–2, and δ-toxin) demonstrated their capacity to self-assemble into fibers (Fig. 6B). We used the amyloid-specific dye thioflavin T (ThT) to observe amyloid formation over time [34,35]. When we assayed the PSMs for polymerization in the presence of ThT at room temperature, we observed a robust increase in normalized
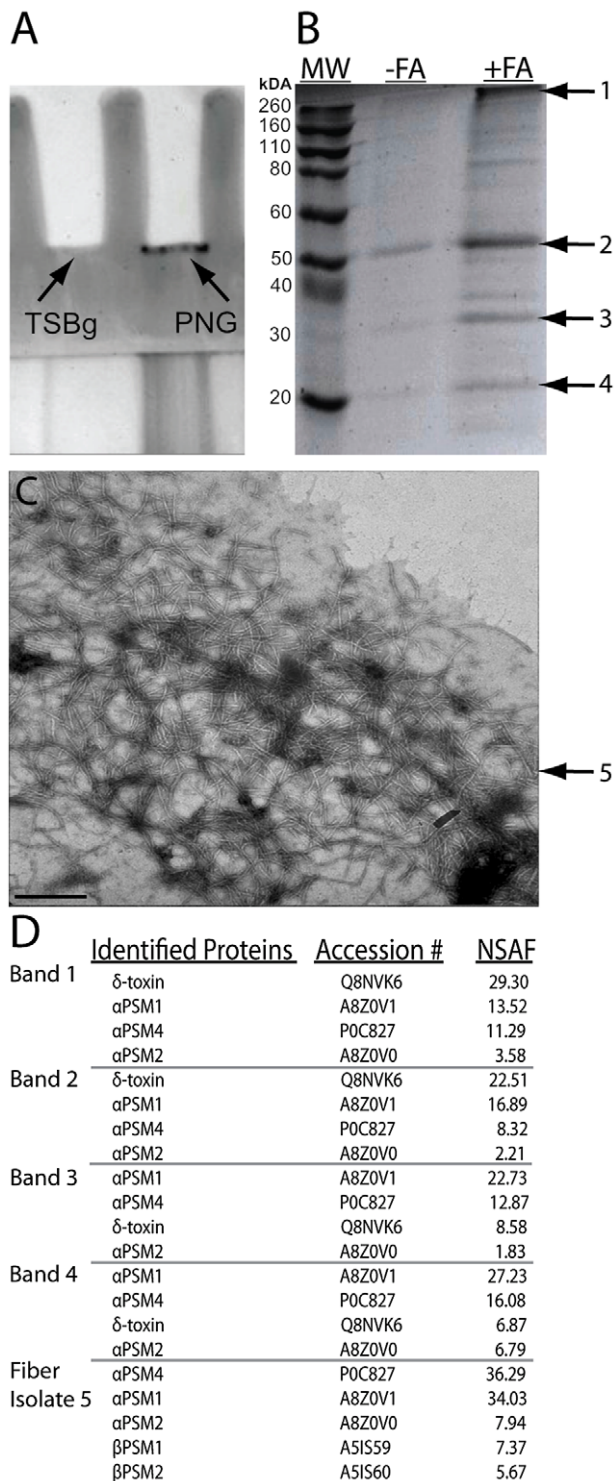
Figure 3. Fibers are composed of phenol soluble modulins. (A) S. aureus biofilm cells were lysed and run into a 12% SDS-PAGE gel (TSBg first lane or PNG second lane); protein that did not migrate through the gel (indicated by arrow) was extracted from the staking gel, treated with formic acid to break up aggregated proteins, and finally run on a new 12% SDS-PAGE gel (B). Bands that appeared after formic acid treatment (1–4) were excised and analyzed via LC-MS/MS. (C) TEM micrograph of purified fiber sample that was then exposed to extensive pepsin digestion and analyzed via LC-MS/MS. Bar indicates 250 nm. (D) Peptides identified by mass spectrometry analysis and their relative abundance factors in the sample (NSAF).
doi:10.1371/journal.ppat.1002744.g003

fluorescence (Fig. 6A). Greater peptide concentration increased ThT fluorescence and showed rapid binding kinetics similar to an amyloid-nucleator system (Fig. 6A) [35,36,37]. PSM fibers exposed to ThT exhibited an emission spike near 490 nm that is also observed in other amyloid fibrils (Fig. 6C) [36,38,39]. Incubation of PSM fibers with the dye Congo red (CR) resulted in a characteristic absorbance "red shift", indicative of cross β structure conserved in all amyloid fibers (Fig. 6D) [40]. Furthermore, PSM fibers isolated from solution through centrifugation displayed increased β-sheet content (Fig. 6E), which is consistent with data published from other bacterial amyloids [13,16]. These in vitro observations compliment our genetic and physiological data, further supporting the notion that PSMs can form amyloid fibrils.

Mutants unable to synthesize PSMs produce biofilms susceptible to matrix-degrading enzymes and mechanical stress

Because biofilms grown in PNG media resist disassembly by matrix-degrading enzymes and surfactants (Fig. 1), we challenged Δαβpsm mutant biofilms grown under the same conditions. In contrast to its isogenic parent strain, an Δαβpsm mutant biofilm readily disassembled after exposure to proteinase K, DNaseI, and dispersin B (Fig. 7A). Complementation of the αβPSM mutant in trans restored the resistant biofilm phenotype (Fig. 7B). We also examined the effects of mechanical stress (vortexing) on biofilms attached at the air-liquid interface of glass culture tubes. An Δαβpsm mutant biofilm readily disassembled with exposure to mechanical stress, while biofilms of the isogenic parent and complemented strains both remained intact (Fig. 7C). Taken together these data do suggest that PSM fibers enhance biofilm integrity.

Fibrilation modulates PSM activity

Previous work has demonstrated that soluble PSMs assist biofilm disassembly [19,21,27]. Based on our findings that PSM fibers improve biofilm integrity (Fig. 1 & Fig. 7), we hypothesized that sequestration of PSMs into extracellular fibers could alter their activity. Synthetic αPSM1 peptides readily formed fibers that bind CR and ThT after 24 hours of incubation in solution (Fig. 8C, 8D, 8E). To test whether or not fibrillation alters peptide activity, we exposed 24-hour S. aureus biofilms to either freshly solublized αPSM1 peptides (Fig. 8B) or αPSM1 that had been allowed to polymerize overnight (Fig. 8C). Exposure to soluble αPSM1 significantly reduced the amount of adherent biofilm; however, exposure to αPSM1 fibers had no discernable effect on the biofilms (Fig. 8A). This finding suggests that the aggregation of PSMs into amyloid-like fibers can modulate their ability to disassemble biofilms.

Discussion

Biofilm formation and disassembly are carefully coordinated with the production and breakdown of matrix components. The biofilm lifecycle of attachment, maturation, and disassembly participates as a mechanism of virulence in many persistent S. aureus infections [1,2,4,5,11,12,19]. A better understanding of the dynamic S. aureus matrix environment may inspire new, innovative techniques for controlling biofilm infections.

Previous studies have shown that the S. aureus biofilm matrix contains polysaccharides and DNA that interact with structural and enzymatic proteins [3,4,5,7,41]. In this work we demonstrate that under certain growth conditions, S. aureus produces amyloid-like fibers that contribute to biofilm integrity (Fig. 1, 2, 7).
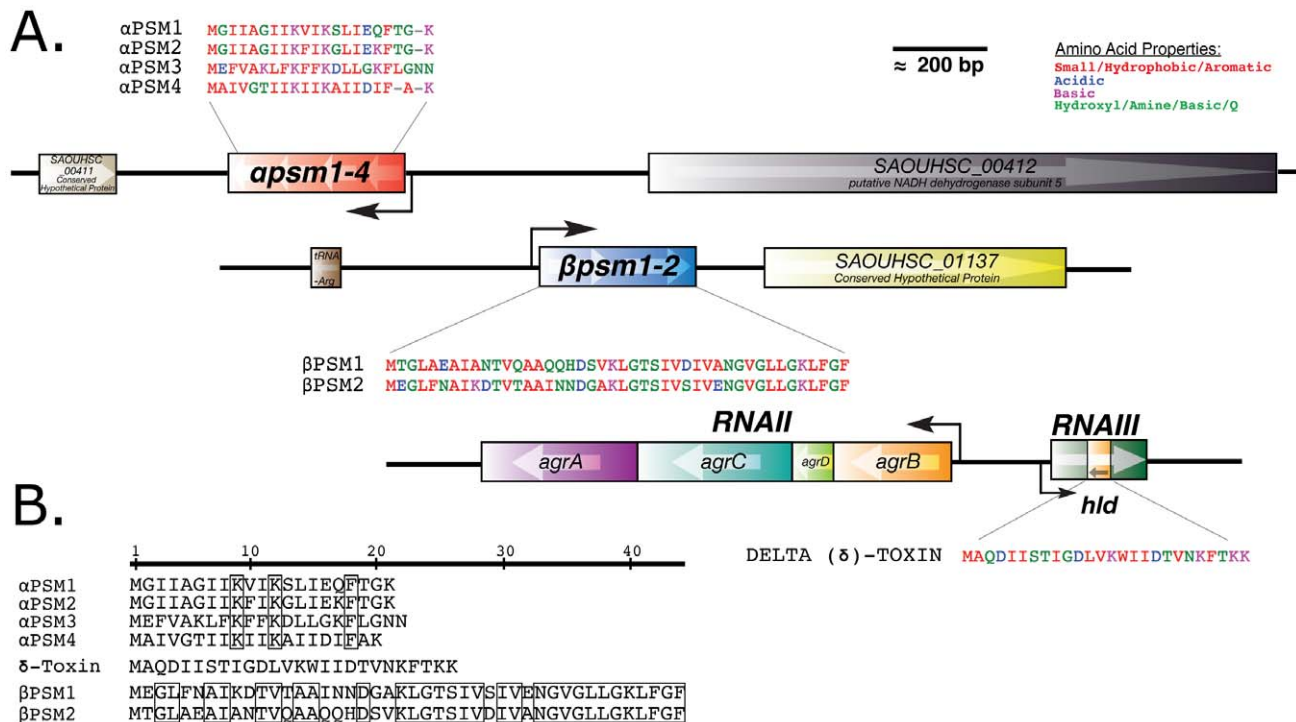
Figure 4. Phenol soluble modulins are small peptides expressed from three discrete regions of the *S. aureus* genome. (A) Phenol soluble modulins (PSMs) are encoded in two operons, the alpha (*αPSM1–4*) and beta (*βPSM1–2*) operons, and δ-toxin is encoded within the Agr regulatory RNA, RNAIII (*hld*). (B) PSMs are small hydrophobic peptides with highly similar amino acid content.
doi:10.1371/journal.ppat.1002744.g004

Purification and analysis of fibers revealed that several small peptides of the phenol soluble modulin family were present (Fig. 3 & Fig. 4). Fibers were not detected in biofilms of an Δ*αβpsm* deletion mutant under the same conditions that favor their production in wildtype strains (Fig. 5). Δ*αβpsm* mutant biofilms

were further demonstrated to be significantly more susceptible to disassembly with matrix degrading enzymes and mechanical stress than their isogenic parent (Fig. 7).

To the best of our knowledge, this is the first report describing an extracellular fibril structure in *S. aureus* biofilms. We refer to
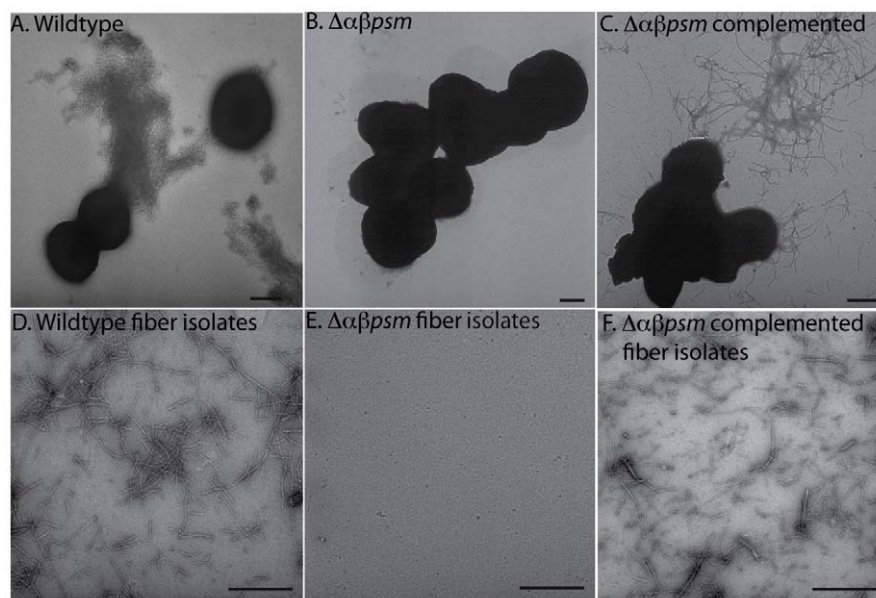
Figure 5. Mutants unable to produce α and βPSMs fail to form fibers during biofilm growth. TEM micrographs of *S. aureus* biofilm cells grown for five days in PNG media. (A) wildtype (strain SH1000), (B) Δ*αβpsm* (strain BB2388), (C) Δ*αβpsm* complemented (strain BB2408). (D–F) TEM micrographs of fiber preparations from wildtype (D), Δ*αβpsm* (E), and Δ*αβpsm* complemented (F). Bars indicate 500 nm.
doi:10.1371/journal.ppat.1002744.g005
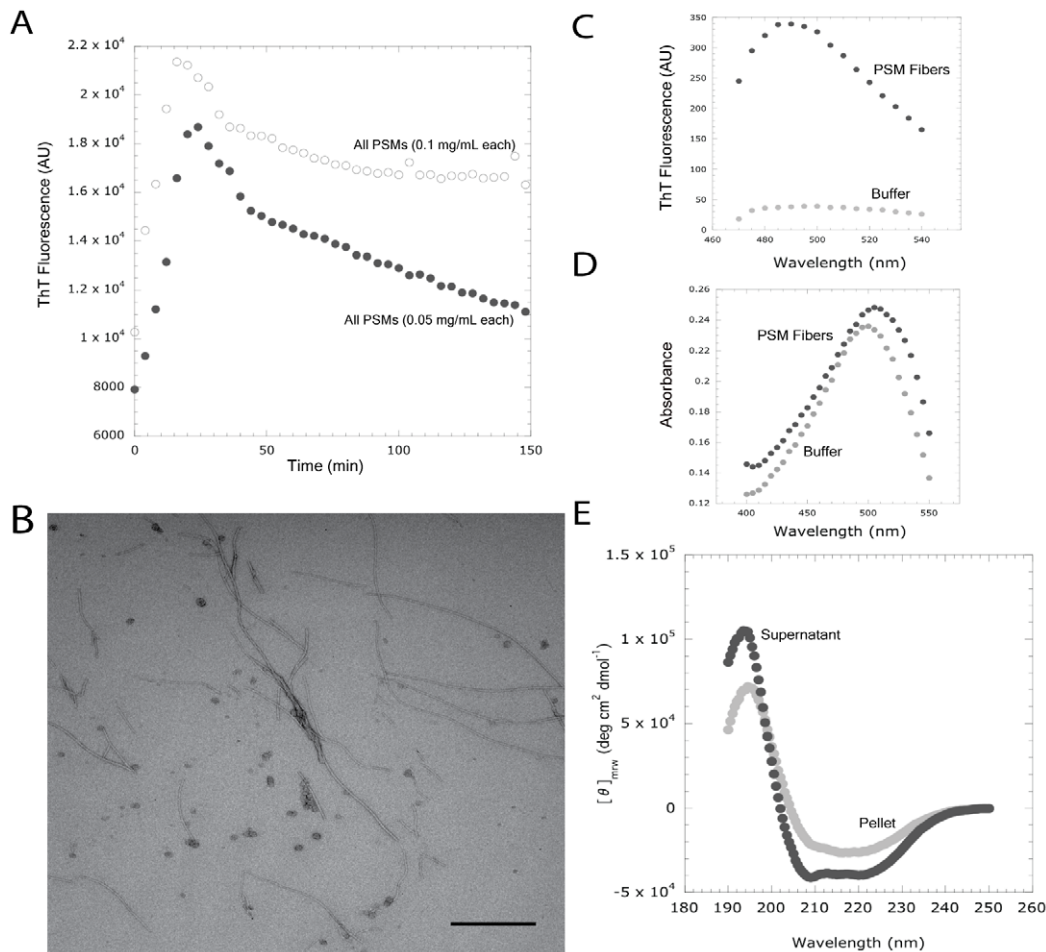
Figure 6. Synthetic phenol soluble modulin peptides bind ThT and polymerize into amyloid-like fibers. (A) Normalized fluorescence intensity of [white circle] 0.1 mg/mL of each PSM peptide or [black circle] 0.05 mg/mL of each PSM peptide in 2 mM ThT. Fluorescence emission was measured at 495 nm after excitation at 438 nm. Assays were repeated in triplicate and all demonstrated a similar trend. (B) 48 hours after mixing 100 μg/mL each of the seven PSM peptides (α1–4, β1–2, and δ-toxin), fibril structures are readily observed by TEM. (C) PSM fibers [black circle] display a ThT fluorescence peak around 482 nm compared to a ThT-only blank [grey circle]. (D) PSM fibers [black circle] produce a characteristic Congo red (CR) absorbance "red-shift" associated with amyloid binding compared to a CR-only blank [grey circle]. (E) Pelleted PSM fibers [grey circle] display a greater β-sheet content than the remaining supernatant [black circle]. Assays were repeated in triplicate and displayed similar trends. Bar indicates 500 nm.

doi:10.1371/journal.ppat.1002744.g006

these matrix components as being amyloid-like because they possess some of the characteristics often attributed to amyloid proteins: fibril morphology (Fig. 2, 5, 6, 8), relative SDS insolubility (Fig. 1 & Fig. 3), binding to the amyloid-specific dyes thioflavin T and Congo red (Fig. 6 & Fig. 8), and they display β-sheet structure [14,31]. The observation that PSM peptides not only self-assemble, but contribute to the biofilm's structural integrity is intriguing in light of recent work describing the PSMs' involvement in biofilm disassembly [11,20,27].

It is well-documented that the PSMs are regulated by the agr quorum-sensing network [11,12,28,42], and we similarly have found that an agr deficient strain did not produce fibers (Fig. 2D). This contributes to a growing body of evidence which implicates the agr system to have wide-ranging effects beyond heightened pathogenicity and biofilm dispersal [4,20,21,43]. It is tempting to speculate that the media-dependent fiber production is somehow influencing agr regulation, perhaps through metabolism or through other signaling cues.

PSMs were first isolated from Staphylococcus epidermidis cultures as a polypeptide complex, and have since been shown to interact

biochemically [22,29]. We have demonstrated that synthetic S. aureus PSM peptides are capable of self-assembling into amyloid-like fibers in vitro (Fig. 6A & Fig. 6B). These fibers demonstrate CR and ThT binding capacities similar to known amyloid proteins. PSMs, including δ-toxin have been previously characterized as amphipathic α helices [22,30,44,45]. Our data indicate that soluble PSMs have a helical structure in solution, but transition to adopt a more β-rich structure after aggregation (Fig. 6E). The assembly of αPSM1 into fibers prevents the biofilm disassembly activity attributed to soluble peptides species (Fig. 7). We interpret these results as evidence that aggregation into amyloid fibers can regulate PSM activity in the microenvironment of the biofilm.

Our findings demonstrate that S. aureus PSMs can be found in biofilms as fibrils, and may implicate fibril formation as a means of altering their activity and function. It is not known at this time what mechanisms influence the PSMs' ability to switch from a monomeric to fibril state, nor is it clear how this affects the formation and disassembly of biofilms. It is possible that PSM fibrillation is synchronized in vivo by a nucleator protein, similar to CsgB in E. coli [34]. Formylation may also play a role; the PSMs
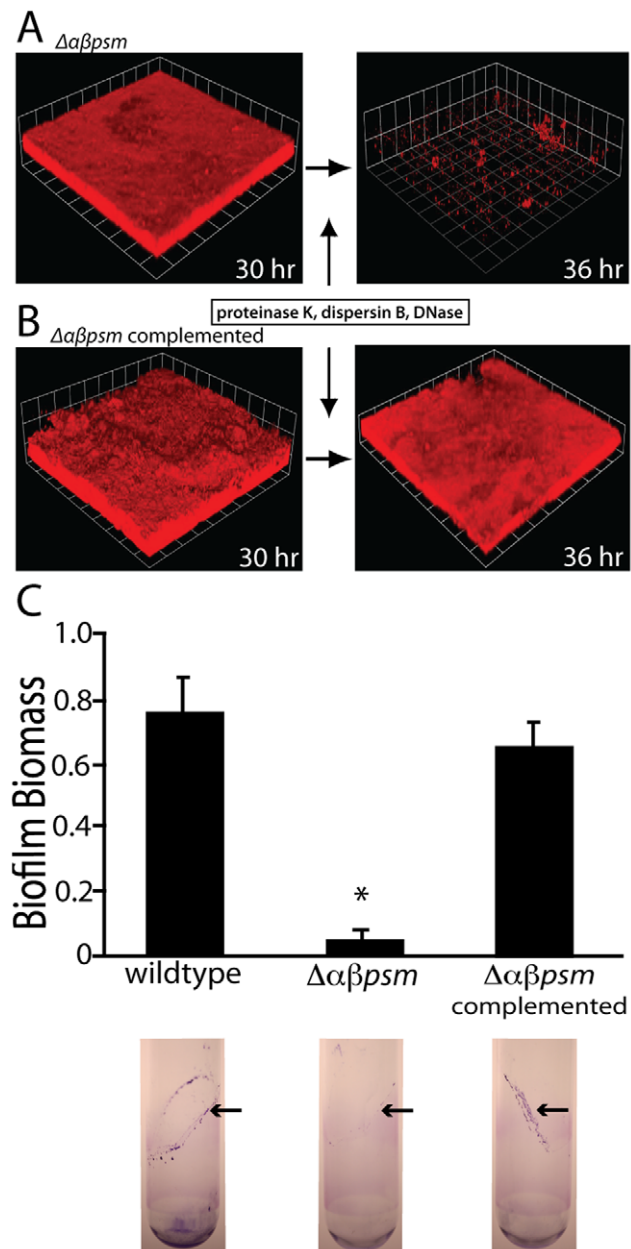
Figure 7. An *αβPSM* **mutant forms biofilms susceptible to disassembly by matrix degrading enzymes and mechanical stress.** Confocal micrographs of Δαβ*psm* mutant (A) (strain BB2388) versus complemented mutant expressing α and β*psm* operons *in trans* (B) (strain BB2408) flow cell biofilms grown for 30 hours prior to proteinase K, dispersin B, and DNaseI exposure (at 0.2 µg/mL each). Images are representative of three separate experiments and each side of a grid square represents 20 µm. (C) Analysis of biofilm development at the air-liquid interface of test tube cultures in PNG media after vortexing. Graph shows quantification of biofilm biomass (OD A_{595}) and images below show stained test tube biofilms. * $P<0.005$ compared to wildtype.

doi:10.1371/journal.ppat.1002744.g007

and δ-toxin are detected at the protein level both with and without with a formylated methionine modification [29,30,46,47], and the PSMs identified in our MS analysis contained primarily deformylated N-methionines. Recent work demonstrates that non-N-formylated PSMs are strong activators of FPR2 receptors, which also respond to amyloidogenic peptides like Aβ_{1-42} and

serum amyloid A [48,49,50], and may implicate a role for deformylation in fibril construction. We speculate that there are numerous other environmental cues (such as pH and osmolarity) driving the PSMs commitment to the fibrillation pathway, and this is currently under investigation.

This study builds upon an emerging paradigm emphasizing that amyloid fibers are common in the biofilm matrices of many bacterial species. Curli fibers produced by pathogenic *E. coli* and other enterics were the first functional amyoloids to be characterized [15,32,33]. The gram-positive bacteria *Streptomyces coelicolor* produces several small peptide species, which have been shown to polymerize *in vitro* and *in vivo* to facilitate sporulation at the air-liquid interface [51,52,53,54]. Recent work in *B. subtilis* has shown that the antimicrobial and spore coat protein TasA can assemble into amyloid-like fibrils during biofilm growth [16]. Even natural biofilms collected from a variety of environmental niches appear to contain amyloid-like fibers [55], indicating that the production of bacterial amyloids may be a shared feature of biofilm matrices from many different bacterial communities.

We propose that amyloid-like aggregation of toxic proteins is an under appreciated form of posttranslational regulation utilized throughout nature, and even more examples continue to emerge. The antimicrobial activity of the *Klebsiella pneumonia* bacteriocin microcin E492 can be turned off through their assembly into amyloid-like fibers [56]. Recent work by Maji *et al.* has demonstrated that even human peptide hormones can form amyloid-like structures for storage [57]. Likewise, PSMs may be stored as inert fibrils in a sessile biofilm until conditions arise that favor their dissociation to promote biofilm disassembly, antimicrobial activity, or virulence. This work presents evidence that *S. aureus* PSMs can be found in biofilms as large fibril structures providing new insight into how quorum sensing and virulence play into the complexity of the biofilm lifecycle.

Materials and Methods

Bacterial strains and growth conditions

The bacterial strains and plasmids used in this study are listed in Table 1. All DNA manipulations were performed in *Escherichia coli* strain DH5α. Oligonucleotides were synthesized by Integrated DNA Technologies (Coralville, IA). Plasmids were transformed into *Staphylococcus aureus* RN4220 by electroporation, purified, and moved to indicated *S. aureus* strains by electroporation. Deletion mutants were generated via allelic replacement using the vector pKFC as described previously [58]. To create the α*psm* mutation, a region upstream of α*psm* was amplified from SH1000 genomic DNA using primers alphaPSM221 (CGC GAG CTC GTT GAG GCA CGC GCC ACT CGC CAG) and alphaPSM162 (GCT AGC GGT ACC ACG CGT GAT GCC AGC GAT GAT ACC CAT TAA) and a downstream region was amplified using alphaPSM163 (ACG CGT GGT ACC GCT AGC TTA AAA TTC TCA GGC CAC TAT ACC) and alphaPSM164 (TAT CCC GGG GAT GGT GGG GGA CTA TCG CGC ACA G). The resulting PCR products were gel purified, digested with KpnI, ligated with T4 DNA ligase and the ligation was used as a template in a subsequent PCR reaction with the primers alphaPSM221 and alphaPSM164. The resulting PCR product was gel purified and digested with SacI and XmaI and ligated with pKFC plasmid digested with the same enzymes to create pKFC-α*psm*. The resulting plasmid construct was used to create an allelic *Δαpsm* deletion in the SH1000 background following the protocol outline by Kato et al [58].

To create the β*psm* mutation, a region upstream of β*psm* was amplified from SH1000 genomic DNA using primers BetaUpF
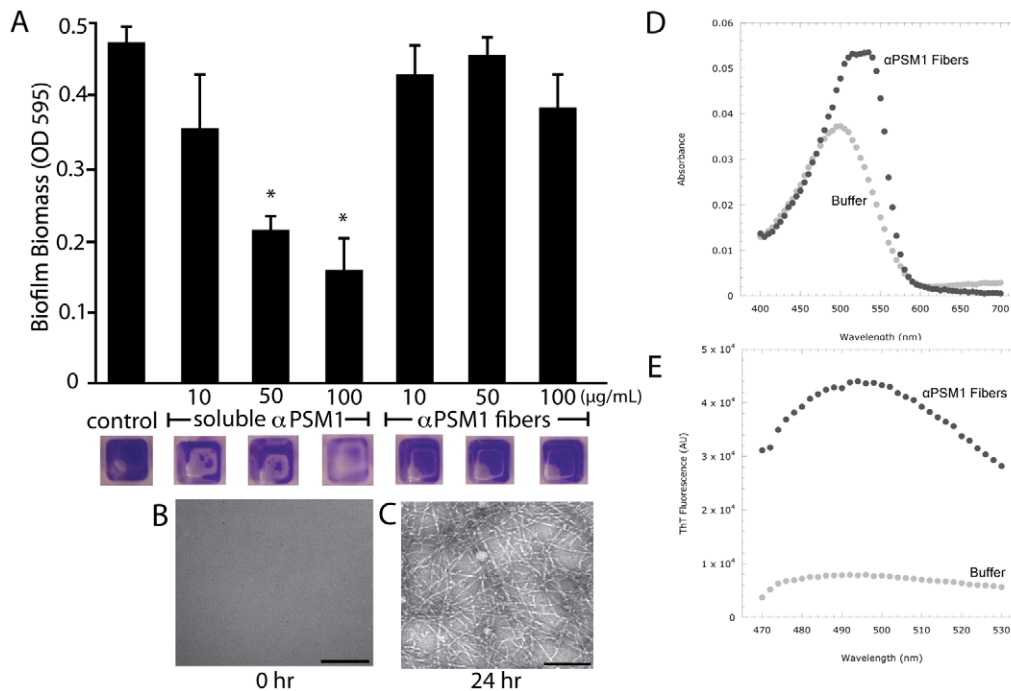
Figure 8. Amyloid fiber formation modulates PSM activity. (A) *S. aureus* wildtype biofilms were grown in microtiter plates for 24 hours then washed and exposed to increasing concentrations of soluble αPSM1 or αPSM1 fibers at concentrations of 10, 50 or 100 μg/mL for six hours. Biofilms were then washed, stained and remaining biofilm biomass was visualized (images of wells below graph) and quantitated (OD at A_{595}). (B & C) TEM micrographs of αPSM1 samples used in the experiment demonstrate the absence (B) and presence (C) of fibers. * $P<0.002$ compared to control no αPSM1 treatment. We verified that αPSM1 fibers bind CR (D) and ThT (E) similar to amyloid fibers.
doi:10.1371/journal.ppat.1002744.g008

(CCC GGA TCC GGT GTA GTG TTG GTG TAG TTC AGG) and BetaUpR (ACG CGT GGT ACC GCT AGC GCG TTA AAT AAA CCT TCC ATT G) and a downstream region was amplified using primers BetaDownF (5′GCT AGC GGT ACC ACG CGT GGC ACA GTT ATC GTA GAC ATC G) and BetaDownR (5′GCG GTC GAC GGC GTC TGA TTT AAC CTT CTC). The resulting PCR products were gel purified and used as a template in a subsequent PCR reaction with the BetaUpF and BetaDownR primers. The resulting PCR product was gel purified and digested with BamHI and SalI and ligated with pKFC plasmid digested with the same enzymes to create pKFC-*βpsm*. The resulting plasmid was used to create an allelic *Δβpsm* deletion in the SH1000 *Δαpsm* background following the protocol outline by Kato et al. to create the double knockout *αβPSM* mutant [58].

Complementation vectors were created as follows: the *βpsm* locus with its native promoter was amplified from *S. aureus* SH1000 genomic DNA using primers GAC GAA TTC AGG CAA CTT AAT TGT G and GAC AAG CTT GCT TCC CAA TGT TGG TG. The resulting PCR product was digested with HindIII and EcoRI and ligated with pAH8 [4], that had been digested with the same enzymes to create pRS*βpsm*. The *αpsm* locus was amplified from SH1000 genomic DNA using primers ACT GAG GTA CCA GAC TCA CCT CAC ATC AAT AA and ACT AGG AGC TCC AAA GGA GGT AAT CTT AAT GGG T. The resulting PCR product was digested with KpnI and SacI and ligated with pALC2073 [59], then digested with the same enzymes to create pALC2073*αPSM*.

Biofilm experiments

Flow cell and drip biofilms were grown as previously described [5,60]. Biofilm growth medium was either 0.6 g/L tryptic soy broth and 1.5 g/L glucose (TSBg) or 3.3 g/L peptone, 2.6 g/L NaCl, 3.3 g/L glucose (PNG).

For biofilm disassembly experiments performed in flow cells, enzymes proteinase K, DNaseI and dispersin B were suspended in water and added to the media reservoir at a final concentration of 0.2 μg/mL. Confocal scanning laser microscopy and image analysis was performed as described previously [5]. Strains contained pAH9 expressing mCherry or were stained with propidium iodide as previously described [5].

Test tube biofilms forming at the air-liquid interface of glass culture tubes were grown in 3 mL of TSBg or PNG for 2 days at 37°C shaking at 200 rpm. Liquid media was removed and exchanged with either 10 mL sterile ddH$_2$O containing 1% SDS or sterile ddH$_2$O alone. Tubes were vortexed for 5 seconds and all liquid was removed. The remaining biofilm biomass was visualized by staining with 0.1% crystal violet and quantified by solublizing the stain in acidified ethanol and measuring the optical density at A_{595}.

Transmission electron microscopy (TEM) was performed using a Philips CM12 transmission electron microscope. Samples prepared for TEM imaging were spotted onto formvar-coated copper grids, incubated for 5 minutes, washed with sterile ddH$_2$O, and negatively stained with 2% uranyl acetate for 60 seconds.

Isolation of fibers from biofilm cultures

Drip bioreactor biofilms were grown as previously described [60]. Fibers were collected after 5 days growth by scraping biofilms into 3 mL of potassium phosphate buffer (50 mM, pH 7). The biofilm suspensions were homogenized using a tissue homogenizer (TissueMiser, Fisher) to shear fibers free from the cell walls. Supernatants were clarified by repeated centrifugation at 13,000 RPM for 2 minutes to remove cells. The cell-free

Table 1. Strains and plasmids used in the present study.

Strain or plasmid	Relevant Genotype	Resistance	Source or reference
Escherichia coli			
DH5α-E	Cloning strain		Invitrogen
Staphylococcus aureus			
RN4220	Restriction modification deficient		[61]
SH1000	Lab strain- σ^{B+} derivative of NCTC8325-4		[62]
SH1001	SH1000 *agr::tet*		[62]
UAMS-1	Osteomylitus isolate		[63]
MN8	Toxic shock isolate		[64]
LAC	CA-MRSA USA300-0114		[65]
AH500	SH1000/pAH9	Erm	[4]
BB606	Blood isolate		This work
BB607	Blood isolate		This work
BB608	Blood isolate		This work
BB862	Nasal isolate		This work
BB863	Nasal isolate		This work
BB864	Nasal isolate		This work
BB2388	SH1000 Δαβ*PSM*		This work
BB2407	Δαβ*PSM*+pALC2073 & pAH8	Erm, Cm	This work
BB2408	Δαβ*PSM*+pALC2073- α*PSM* & pRSβ*PSM*	Erm, Cm	This work
Plasmids			
pAH8	*agr* promoter P$_3$-RFP	Amp, Erm	[4]
pALC2073	*agr* promoter P$_3$-RFP	Cm	[66]
pALC2073 - α*PSM*	α*PSM* locus under control of tet promoter	Cm	This work
pRS - β*PSM*	β*PSM* locus under control of native promoter in pRS10	Amp, Erm	This work
pKFC	Gene replacement vector	Amp, Tet	[58]
pKFC- α*PSM*	α*PSM* knockout vector	Amp, Tet	This work
pKFC- β*PSM*	β*PSM* knockout vector	Amp, Tet	This work

doi:10.1371/journal.ppat.1002744.t001

supernatant was incubated in 200 mM NaCl and the fibers were isolated using Millipore Amicon Ultra Centrifugal Filter Units with a pore size of 100 kDa. Presence of fibers was confirmed via TEM imaging.

Identification of aggregative peptides

Fibril subunits were identified by harvesting drip biofilms after 5 days of growth in PNG and suspending them in 15 mL 10 mM Tris HCl, pH 8.0 (Tris buffer), supplemented with 0.1 mg of RNase A (bovine pancreas; Sigma Chemical Co., St. Louis, Mo.) and 0.1 mg of DNaseI (bovine pancreas; Boehringer, Mannheim, Germany) per mL. Cells were lysed by repeated sonication and the addition of lysostaphin (1 mg/mL, Sigma) and 1 mM MgCl$_2$ prior to incubation at 37°C for 20 min. Lysozyme (Sigma) was added to 1 mg/mL, and the samples were incubated with shaking for 40 min at 37°C, after which they were adjusted to 1% sodium dodecyl sulfate (SDS) and incubated further (30 min, 37°C). The remaining insoluble material was collected by centrifugation (12,100×g, 15 min, 25°C), washed and suspended in 10 mL 10 mM Tris buffer. The pellet was digested again with RNase, DNaseI, and lysostaphin as described above, washed twice with Tris buffer, and suspended in 2 mL SDS-polyacrylamide gel electrophoresis (PAGE) sample buffer (10% glycerol, 5%-mercap-toethanol, 1% SDS, 62.5 mM Tris HCl [pH 6.8]). The sample was boiled for 5 min, loaded onto a 12% polyacrylamide gel (3% stacking gel), and subjected to electrophoresis at 20 mA for 5 h. The material retained in the stacking gel was excised, washed three times in ddH$_2$0, extracted twice with 95% ethanol, and dried in a speedvac. The desiccated sample was resuspended in ddH$_2$0 and sonicated to break up any clumps. Half of this material was incubated with formic acid (90%) for 20 min then dried in a speedvac. Both the formic acid treated and untreated samples were resuspended in SDS-PAGE sample buffer and run into a fresh 12% PAGE gel. Bands that appeared in the formic acid treated sample were excised and analyzed via LC-MS/MS (MS Bioworks, Ann Arbor, MI).

Fiber protein components were also identified by incubating fiber isolates in pepsin for 24 h before subsequent LC-MS/MS analysis (MS Bioworks, Ann Arbor, MI). The value for the abundance measurement is the Normalized Spectral Abundance Factor (NSAF).

PSM polymerization experiments

Non-formylated PSM peptides were synthesized by Peptide 2.0 and assayed to be >90% pure by HPLC. Synthetic peptides were prepared and assayed as previously described [15,34] to eliminate

large aggregates from lyophilization prior to assay. Each dry peptide stock was dissolved to a concentration of 0.5 mg/mL in a 1:1 mixture of trifluoroacetic acid (TFA) and hexafluoroisopropanol (HFIP). Peptides were then sonicated for 10 minutes and incubated at room temperature for 1 h. Solvent TFA/HFIP was removed by speedvac at room temperature. Dried peptide stocks were stored at −80°C. All assays were performed with equal stoichiometric ratios of 0.1 mg/mL peptide unless otherwise noted.

All polymerization assays were performed in 96-well black opaque, polystyrene, TC-treated plates (Corning). Prior to assay, treated peptides were thawed and dissolved in dimethyl sulfoxide (DMSO) to a concentration of 10 mg/mL immediately prior to assay. Freshly dissolved peptides were diluted into sterile ddH$_2$O containing 0.2 mM thioflavin T (ThT) and assayed at room temperature. Fluorescence was measured every 10 minutes after shaking by a Tecan Infinite M200 plate reader at 438 nm excitation and 495 nm emission. ThT fluorescence during polymerization was corrected by subtracting the background intensity of an identical sample without ThT.

Additionally, ThT fluorescence and Congo red (CR) absorbance scans were performed on polymerized peptides that were allowed to polymerize for 48 h in ddH$_2$O. Samples were incubated in 0.2 mM ThT or 0.001% (w/v) CR in ddH$_2$O for 15 minutes prior to assay on the Tecan plate reader. CR and ThT scans were corrected by subtracting the background intensity of an identical sample without dye.

Circular dichroism spectroscopy

Treated peptide stocks were thawed and dissolved in hexafluoroisopropanol (HFIP) to a concentration of 10 mg/mL immediately prior to assay. Triplicate samples consisting of 0.1 mg/mL of each freshly dissolved peptide diluted together in 500 μL sterile ddH$_2$O were incubated with shaking at room temperature for 48 h. Samples were then pelleted at 15,000 RPM for 30 minutes to isolate any aggregated species. The supernatant was carefully removed from the pellet by aspiration and transferred to a clean, sterile eppendorf tube. The remaining pellet was resuspended in 200 μL ddH$_2$O by bath sonication for 10 minutes. The supernatant and pellets of each sample were assayed separately. Far UV circular dichroism (CD) measurements were performed with a Jasco-J715 spectropolarimeter using quartz cells with 0.1 cm path length. CD spectra between 190 and 250 nm were recorded in millidegrees and converted to molar ellipticity using an average MRW of 113 for αPSM1–4, βPSM1&2, and δ-toxin. The average of five scans was recorded at 25°C using a 2 nm bandwidth with a 20 nm min^{-1} scanning speed. All triplicate samples showed similar ellipticity patterns.

Biofilm dispersal assay

Synthetic PSM peptides were allowed to polymerize overnight, and fibril formation was verified by TEM imaging. Equivalent concentrations of either polymerized or freshly diluted peptides were added to 24 hours SH1000 biofilms grown in 66% TSB+0.2% glucose and incubated at 37°C for 6 hours. Biofilms were washed to remove non-adherent cells then stained with 0.1% crystal violet, dried, and solublized with acidified ethanol and spectroscopically quantitated at A$_{595}$.

Statistics were performed using a 1-way analysis of variance (ANOVA). Results are expressed as mean ± standard deviation.

Acknowledgments

Author Contributions

Conceived and designed the experiments: KS AKS RES BRB. Performed the experiments: KS AKS RES AHR BRB. Analyzed the data: KS AKS RES BRB. Contributed reagents/materials/analysis tools: AHR. Wrote the paper: KS BRB.

References

1. Otto M (2008) Staphylococcal biofilms. Curr Top Microbiol Immunol 322: 207–228.
2. Boles BR, Horswill AR (2011) Staphylococcal biofilm disassembly. Trends Microbiol 19: 449–455.
3. Izano EA, Amarante MA, Kher WB, Kaplan JB (2008) Differential roles of poly-N-acetylglucosamine surface polysaccharide and extracellular DNA in Staphylococcus aureus and Staphylococcus epidermidis biofilms. Appl Environ Microbiol 74: 470–476.
4. Lauderdale KJ, Boles BR, Cheung AL, Horswill AR (2009) Interconnections between Sigma B, agr, and proteolytic activity in Staphylococcus aureus biofilm maturation. Infect Immun 77: 1623–1635.
5. Boles BR, Horswill AR (2008) Agr-mediated dispersal of Staphylococcus aureus biofilms. PLoS Pathog 4: e1000052.
6. Mann EE, Rice KC, Boles BR, Endres JL, Ranjit D, et al. (2009) Modulation of eDNA release and degradation affects Staphylococcus aureus biofilm maturation. PLoS ONE 4: e5822.
7. Boles BR, Thoendel M, Roth AJ, Horswill AR (2010) Identification of genes involved in polysaccharide-independent Staphylococcus aureus biofilm formation. PLoS ONE 4: e10146.
8. Zhu Y, Weiss EC, Otto M, Fey PD, Smeltzer MS, et al. (2007) Staphylococcus aureus biofilm metabolism and the influence of arginine on polysaccharide intercellular adhesin synthesis, biofilm formation, and pathogenesis. Infect Immun 75: 4219–4226.
9. Lindsay JA, Moore CE, Day NP, Peacock SJ, Witney AA, et al. (2006) Microarrays reveal that each of the ten dominant lineages of Staphylococcus aureus has a unique combination of surface-associated and regulatory genes. J Bacteriol 188: 669–676.
10. Resch A, Rosenstein R, Nerz C, Gotz F (2005) Differential Gene Expression Profiling of Staphylococcus aureus Cultivated under Biofilm and Planktonic Conditions. Appl Environ Microbiol 71: 2663–2676.
11. Vuong C, Saenz HL, Gotz F, Otto M (2000) Impact of the agr quorum-sensing system on adherence to polystyrene in Staphylococcus aureus. J Infect Dis 182: 1688–1693.
12. Cassat J, Dunman PM, Murphy E, Projan SJ, Beenken KE, et al. (2006) Transcriptional profiling of a Staphylococcus aureus clinical isolate and its isogenic agr and sarA mutants reveals global differences in comparison to the laboratory strain RN6390. Microbiology 152: 3075–3090.
13. Dueholm MS, Petersen SV, Sonderkaer M, Larsen P, Christiansen G, et al. (2010) Functional amyloid in Pseudomonas. Mol Microbiol 77: 1009–1020.
14. Gebbink MFBG, Claessen D, Bouma B, Dijkhuizen L, Wosten HAB (2005) Amyloids - A functional coat for microorganisms. Nat Rev Microbiol 3: 333–341.
15. Chapman MR, Robinson LS, Pinkner JS, Roth R, Heuser J, et al. (2002) Role of Escherichia coli curli operons in directing amyloid fiber formation. Science 295: 851–855.
16. Romero D, Aguilar C, Losick R, Kolter R (2010) Amyloid fibers provide structural integrity to Bacillus subtilis biofilms. Proc Natl Acad Sci U S A 107: 2230–2234.
17. Vuong C, Gotz F, Otto M (2000) Construction and characterization of an agr deletion mutant of Staphylococcus epidermidis. Infect Immun 68: 1048–1053.
18. Queck SY, Khan BA, Wang R, Bach THL, Kretschmer D, et al. (2009) Mobile genetic element-encoded cytolysin connects virulence to methicillin resistance in MRSA. PLoS Pathog 5: e1000533.
19. Kong K-F, Vuong C, Otto M (2006) Staphylococcus quorum sensing in biofilm formation and infection. Int J Med Microbiol 296: 133–139.
20. Tsompanidou E, Sibbald MJ, Chlebowicz MA, Dreisbach A, Back JW, et al. (2011) Requirement of the agr locus for colony spreading of Staphylococcus aureus. J Bacteriol 193: 1267–1272.
21. Periasamy S, Joo HS, Duong AC, Bach TH, Tan VY, et al. (2012) How Staphylococcus aureus biofilms develop their characteristic structure. Proc Natl Acad Sci U S A 109: 1281–1286.
22. Cogen AL, Yamasaki K, Sanchez KM, Dorschner RA, Lai Y, et al. (2009) Selective Antimicrobial Action Is Provided by Phenol-Soluble Modulins Derived from Staphylococcus epidermidis, a Normal Resident of the Skin. J Invest Dermatol 130: 192–200.

23. Cogen AL, Yamasaki K, Muto J, Sanchez KM, Alexander LC, et al. (2010) *Staphylococcus epidermidis* Antimicrobial δ-Toxin (Phenol-Soluble Modulin-γ) Cooperates with Host Antimicrobial Peptides to Kill Group A *Streptococcus*. PLoS ONE 5: e8557.

24. Marchand A, Verdon J, Lacombe C, Crapart S, Hechard Y, et al. (2011) Anti-*Legionella* activity of staphylococcal hemolytic peptides. Peptides 32: 845–851.

25. Diep B, Otto M (2008) The role of virulence determinants in community-associated MRSA pathogenesis. Trends Microbiol 16: 361–369.

26. Kaito C, Saito Y, Nagano G, Ikuo M, Omae Y, et al. (2011) Transcription and Translation Products of the Cytolysin Gene *psm-mec* on the Mobile Genetic Element SCC*mec* Regulate *Staphylococcus aureus* Virulence. PLoS Pathog 7: e1001267.

27. Wang R, Khan BA, Cheung GYC, Bach T-HL, Jameson-Lee M, et al. (2011) *Staphylococcus epidermidis* surfactant peptides promote biofilm maturation and dissemination of biofilm-associated infection in mice. J Clin Invest 121: 238–248.

28. Janzon L, Lofdahl S, Arvidson S (1989) Identification and nucleotide sequence of the delta-lysin gene, *hld*, adjacent to the accessory gene regulator (*agr*) of *Staphylococcus aureus*. Mol Gen Genet 219: 480–485.

29. Mehlin C, Headley CM, Klebanoff SJ (1999) An inflammatory polypeptide complex from *Staphylococcus epidermidis*: isolation and characterization. J Exp Med 189: 907–918.

30. Wang R, Braughton KR, Kretschmer D, Bach T-HL, Queck SY, et al. (2007) Identification of novel cytolytic peptides as key virulence determinants for community-associated MRSA. Nat Med 13: 1510–1514.

31. Fowler DM, Koulov AV, Balch WE, Kelly JW (2007) Functional amyloid–from bacteria to humans. Trends Biochem Sci 32: 217–224.

32. Nielsen PH, Dueholm MS, Thomsen TR, Nielsen JL, Otzen D (2011) Functional Bacterial Amyloids in Biofilms. In: Flemming H-C et al. editors. Biofilm Highlights, Springer Series on Biofilms Springer-Verlag, Berlin. pp 5, 41–62.

33. Collinson SK, Emody L, Muller KH, Trust TJ, Kay WW (1991) Purification and characterization of thin, aggregative fimbriae from. J Bacteriol 173: 4773–4781.

34. Wang X, Zhou Y, Ren J-J, Hammer ND, Chapman MR (2010) Gatekeeper residues in the major curlin subunit modulate bacterial amyloid fiber biogenesis. Proc Natl Acad Sci U S A 107: 163–168.

35. Wang X, Smith DR, Jones JW, Chapman MR (2007) *In vitro* polymerization of a functional *Escherichia coli* amyloid protein. J Biol Chem 282: 3713–3719.

36. Groenning M, Olsen L, van de Weert M, Flink JM, Frokjaer S, et al. (2007) Study on the binding of Thioflavin T to β-sheet-rich and non-β-sheet cavities. J Struct Biol 158: 358–369.

37. Hammer ND, Wang X, McGuffie BA, Chapman MR (2008) Amyloids: friend or foe? J Alzheimers Dis 13: 407–419.

38. LeVine H, 3rd (1993) Thioflavine T interaction with synthetic Alzheimer's disease β-amyloid peptides: detection of amyloid aggregation in solution. Protein Sci 2: 404–410.

39. Biancalana M, Koide S (2010) Molecular mechanism of Thioflavin-T binding to amyloid fibrils. Biochim Biophys Acta 1804: 1405–1412.

40. Klunk WE, Jacob RF, Mason RP (1999) Quantifying amyloid by congo red spectral shift assay. Methods Enzymol 309: 285–305.

41. Vuong C, Kocianova S, Voyich JM, Yao Y, Fischer ER, et al. (2004) A crucial role for exopolysaccharide modification in bacterial biofilm formation, immune evasion, and virulence. J Biol Chem 279: 54881–54886.

42. Queck SY, Jameson-Lee M, Villaruz AE, Bach T-HL, Khan BA, et al. (2008) RNAIII-independent target gene control by the *agr* quorum-sensing system: insight into the evolution of virulence regulation in *Staphylococcus aureus*. Mol Cell 32: 150–158.

43. Yarwood JM, Bartels DJ, Volper EM, Greenberg EP (2004) Quorum sensing in *Staphylococcus aureus* biofilms. J Bacteriol 186: 1838–1850.

44. Dhople VM, Nagaraj R (2005) Conformation and activity of δ-lysin and its analogs. Peptides 26: 217–225.

45. Talbot JC, Thiaudiere E, Vincent M, Gallay J, Siffert O, et al. (2001) Dynamics and orientation of amphipathic peptides in solution and bound to membranes: a steady-state and time-resolved fluorescence study of staphylococcal δ-toxin and its synthetic analogues. Eur Biophys J 30: 147–161.

46. Jones RC, Deck J, Edmondson RD, Hart ME (2008) Relative Quantitative Comparisons of the Extracellular Protein Profiles of *Staphylococcus aureus* UAMS-1 and Its *sarA*, *agr*, and *sarA agr* Regulatory Mutants Using One-Dimensional Polyacrylamide Gel Electrophoresis and Nanocapillary Liquid Chromatography Coupled with Tandem Mass Spectrometry. J Bacteriol 190: 5265–5278.

47. Somerville GA, Cockayne A, Durr M, Peschel A, Otto M, et al. (2003) Synthesis and deformylation of *Staphylococcus aureus* δ-toxin are linked to tricarboxylic acid cycle activity. J Bacteriol 185: 6686–6694.

48. Tiffany HL, Lavigne MC, Cui YH, Wang JM, Leto TL, et al. (2001) Amyloid-β induces chemotaxis and oxidant stress by acting at formyl peptide receptor 2, a G protein-coupled receptor expressed in phagocytes and brain. J Biol Chem 276: 23645–23652.

49. Kretschmer D, Gleske AK, Rautenberg M, Wang R, Koberle M, et al. (2010) Human formyl peptide receptor 2 senses highly pathogenic *Staphylococcus aureus*. Cell Host Microbe 7: 463–473.

50. Rautenberg M, Joo HS, Otto M, Peschel A (2011) Neutrophil responses to staphylococcal pathogens and commensals via the formylpeptide receptor 2 relates to phenol-soluble modulin release and virulence. FASEB J 25: 1254–1263.

51. Claessen D, Rink R, de Jong W, Siebring J, de Vreugd P, et al. (2003) A novel class of secreted hydrophobic proteins is involved in aerial hyphae formation in *Streptomyces coelicolor* by forming amyloid-like fibrils. Genes Dev 17: 1714–1726.

52. de Jong W, Wösten HAB, Dijkhuizen L, Claessen D (2009) Attachment of *Streptomyces coelicolor* is mediated by amyloidal fimbriae that are anchored to the cell surface via cellulose. Mol Micro 73: 1128–1140.

53. Sawyer EB, Claessen D, Haas M, Hurgobin B, Gras SL (2011) The Assembly of Individual Chaplin Peptides from *Streptomyces coelicolor* into Functional Amyloid Fibrils. PLoS ONE 6: e18839.

54. Capstick DS, Jomaa A, Hanke C, Ortega J, Elliot MA (2011) Dual amyloid domains promote differential functioning of the chaplin proteins during *Streptomyces* aerial morphogenesis. Proc Natl Acad Sci U S A 108: 9821–9826.

55. Larsen P, Nielsen JL, Dueholm MS, Wetzel R, Otzen D, et al. (2007) Amyloid adhesins are abundant in natural biofilms. Environ Microbiol 9: 3077–3090.

56. Bieler S, Estrada L, Lagos R, Baeza M, Castilla J, et al. (2005) Amyloid formation modulates the biological activity of a bacterial protein. J Biol Chem 280: 26880–26885.

57. Maji SK, Perrin MH, Sawaya MR, Jessberger S, Vadodaria K, et al. (2009) Functional amyloids as natural storage of peptide hormones in pituitary secretory granules. Science 325: 328–332.

58. Kato F, Sugai M (2011) A simple method of markerless gene deletion in *Staphylococcus aureus*. J Microbiol Methods 87: 76–81.

59. Corrigan RM, Foster TJ (2009) An improved tetracycline-inducible expression vector for *Staphylococcus aureus*. Plasmid 61: 126–129.

60. Schwartz K, Stephenson R, Hernandez M, Jambang N, Boles BR (2010) The use of drip flow and rotating disk reactors for *Staphylococcus aureus* biofilm analysis. J Vis Exp. pii: 2470. doi: 10.3791/2470.

61. Kreiswirth BN, Lofdahl S, Betley MJ, O'Reilly M, Schlievert PM, et al. (1983) The toxic shock syndrome exotoxin structural gene is not detectably transmitted by a prophage. Nature 305: 709–712.

62. Horsburgh MJ, Aish JL, White IJ, Shaw L, Lithgow JK, et al. (2002) σ^B modulates virulence determinant expression and stress resistance: characterization of a functional *rsbU* strain derived from *Staphylococcus aureus* 8325-4. J Bacteriol 184: 5457–5467.

63. Gillaspy AF, Hickmon SG, Skinner RA, Thomas JR, Nelson CL, et al. (1995) Role of the accessory gene regulator (*agr*) in pathogenesis of staphylococcal osteomyelitis. Infect Immun 63: 3373–3380.

64. Maira-Litran T, Kropec A, Abeygunawardana C, Joyce J, Mark G, 3rd, et al. (2002) Immunochemical properties of the staphylococcal poly-*N*-acetylglucosamine surface polysaccharide. Infect Immun 70: 4433–4440.

65. Voyich JM, Braughton KR, Sturdevant DE, Whitney AR, Said-Salim B, et al. (2005) Insights into mechanisms used by *Staphylococcus aureus* to avoid destruction by human neutrophils. J Immunol 175: 3907–3919.

66. Bateman BT, Donegan NP, Jarry TM, Palma M, Cheung AL (2001) Evaluation of a tetracycline-inducible promoter in *Staphylococcus aureus* in vitro and in vivo and its application in demonstrating the role of *sigB* in microcolony formation. Infect Immun 69: 7851–7857.